Specific ion effects in non-aqueous solvents:

the case of glycerol carbonate

Filippo Sarri,[1] Duccio Tatini,[1] Damiano Tanini,[1] Matteo Simonelli,[1] Moira Ambrosi,[1] Barry W. Ninham,[2] Antonella Capperucci,[1] Luigi Dei,[1] and Pierandrea Lo Nostro*[1]

1: Department of Chemistry "Ugo Schiff" and CSGI, University of Florence, Via della Lastruccia 3, 50019 Sesto Fiorentino (Firenze), Italy

2: Department of Applied Mathematics, Research School of Physical Sciences and Engineering, Australian National University, Canberra ACT 0200, Australia

_____

*: corresponding author. Email: pierandrea.lonostro@unifi.it - Phone: +39 055 4573010.

1 **Abstract**

2 The effect of eight potassium salts (KF, K_3PO_4, KOCN, K_2CO_3, KCl, K_2SO_4, KBr and

3 KI) on glycerol carbonate (GC) is studied through NMR, DSC, solubility and ATR-

4 FTIR experiments. From the solubility data, the main thermodynamic functions of

5 solution and solvation are estimated, and the mean molal activity coefficients are

6 calculated. The results suggest that the capability of an anion to establish hydrogen

7 bonds with the solvent molecules (or behave as a base, as in the case of fluoride,

8 phosphate, cyanate and carbonate) is the most important structural feature that

9 determines its effects on the solvent structure. On the other hand potassium iodide

10 behaves in an anomalous way, due to the large polarizability of the anion that can

11 form non-electrostatic, van der Waals dispersive intermolecular interactions.

12

13 **Keywords.**

14 Hofmeister series; specific ion effect; ion pairs; glycerol carbonate

15

1 Introduction

In a previous paper [1] we reported some curious effects that followed saturation of glycerol carbonate (GC) with potassium fluoride. The effects were studied at room temperature via conductivity, rheology, differential scanning calorimetry (DSC) and attenuated total reflection Fourier-transform infrared spectroscopy (ATR-FTIR) measurements. We found that KF forms mainly ion pairs, triple ions and larger clusters. Together with a few free ions these impart to the thixotropic solvent a structuredness much stronger than expected for the mixture. Apparently this occurs through the formation of hydrogen bonds (HB) with the fluoride anion and ion-dipole interactions between K^+ and the carbonyl residue [1].

Here we extend the previous work to include the solubility and behavior of a range of other potassium salts in GC. We compare the results with those for other cyclic carbonates previously explored. Since we operate either at the saturation limit or at a moderately high concentration our results are both anion and solvent specific. The aim is to explore the nature of non- aqueous solvent Hofmeister effects systematically. To do so, information on variation of the thermodynamics of solvation across a range of solvents, the effect of ions on solvent structure and on solvent dynamics need to be available to obtain a comprehensive physical picture [2].

Alkylene carbonates such as GC, propylene carbonate (PC) and ethylene carbonate (EC) are non-aqueous associated liquids with strong van der Waals intermolecular interactions as suggested by their structural features (see Scheme 1), and by some of their physico-chemical properties (see Table 1) [3,4].
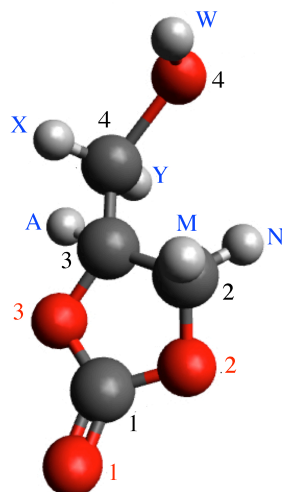
1
2 **Scheme 1.** Minimized chemical structure of GC. Grey, red and white spheres
3 represent carbon, oxygen and hydrogen atoms, respectively. In blue the numbering for
4 hydrogens, in black the numbering for carbons, and in red the numbering for oxygens.
5 Partial charges (calculated with Avogadro 1.1.0): C1: +0.511, C2: +0.135, C3:
6 +0.163, C4: +0.085, O1: -0,203 O2: -0.430, O3: -0.425, O4: -0.391, H_M: +0.074, H_N:
7 +0.074, : H_A: +0.079, H_X: +0.060, H_Y: +0.060, H_W: +0.210.
8

9 **Table 1**. Physico-chemical properties of glycerol, propylene and ethylene carbonate
10 at 25 °C. In the case of GC the phase change refers to a glass transition.

Property	GC	PC	EC[a]	H_2O
Dielectric constant, ε	109.7	64.9	89.8	80.1
Dipole moment, μ (D)[b]	5.05	5.36	4.81	1.85
Viscosity, η (cP)	85.4[c]	2.53	1.90	0.89
Surface tension, γ (mN/m)	44.2	34.6[j]	50.6[a]	72
Heat capacity, C_p(liquid) (J/mol·K)	201[g]	170[g]	156[h]	75.29
Melting point, mp (° C)	(-70.8°)	-52.7°	38.2°	0°
Fusion enthalpy, $\Delta_{fus}H$ (kJ/mol)	(19.6)[i]	8.96[f]	13.02[f]	6.01
Fusion entropy, $\Delta_{fus}S$ (J/mol·K)	(97)	41	43	22
Boiling point, bp (° C)	354°	242	248°	100°
Vaporization enthalpy, $\Delta_{vap}H$ (kJ/mol)	78.5	56.3[e]	55.2[e]	40.66
Vaporization entropy, $\Delta_{vap}S$ (J/mol·K)	125	109	107	109
Static polarizability, α_0 (Å³)[k]	9.3[l]	8.5[l]	6.6[l]	1.5[m]

11 a: at 40° C. b: from Ref. 5. c: from Ref. 6. d: this work. e: at 150° C, from Ref. 7. f:
12 from Refs. 8 and 9. g: at 30° C from Ref. 5. h: at 110° C from Ref. 5. i: calculated
13 from Ref. 10. j: from Ref. 11. k: experimental values obtained from the Lorenz-
14 Lorentz equation. l: from Ref. 12. m: from Ref. 13.
15
16

17 All solvents considered in Table 1 possess high dielectric constants and dipole

18 moments. The conventional view is that this explains why alkylene carbonates are

19 suitable solvents for strong electrolytes and therefore widely used in different

1 industrial areas [5,6]. Solvent-solvent and salt-solvent intermolecular interactions are

2 often depicted in a too simplistic view that derives from an electrostatic (Born energy)

3 interpretation of free energies of ion transfer. We now know that dispersion self

4 energies provide significant ion specific contributions [14-21].

5 Alkylene carbonates (glycerol, ethylene and propylene carbonates) also possess high

6 heat capacities and large phase transition parameters that reflect the strong

7 intermolecular interactions.

8 In the case of GC a terminal primary -OH residue further increases the ordered

9 structure of the solvent and can assist in the ion solvation through hydrogen bonding

10 (HB). Scheme 1 shows the atom numbering and the partial charge on each atom in

11 GC. The presence of a significant negative charge on the carbonyl oxygen (O1) that

12 can strongly interact with the terminal hydroxyl group on the other side of the

13 molecule and build up a robust structuredness in the liquid, as reflected by some

14 solvent properties such as the high enthalpy of vaporization and the relatively low

15 enthalpy of melting. Moreover GC possesses a large static polarizability (about 9.3

16 Å^3, see Ref. 12), larger than that of PC and EC (see Table 1), that – together with the

17 large dipole moment - can justify the existence of important and highly cooperative

18 van der Waals intermolecular interactions [22].

19 Another consequence of their ordered structure is that molecular liquids like

20 GC and PC behave as excellent low-molecular-weight organic glass formers,

21 [23-25]. In fact these materials show non-liquid-like features, such as the

22 rheological behavior typical of a soft glass, that make them very interesting for

23 fundamental research and technological applications [26,27]. In spite of the

24 increasing interest in innovative synthetic routes of GC in order to cut the

1 production costs and enhance the yield [28,29], only few articles on the GC

2 physico-chemical properties have appeared in the literature [30].

3 This is suprising because several applications take advantage of the properties

4 of GC. These include for example the technology of lithium and lithium-ion

5 batteries, cement and concrete industries, sugar cane treatment, cosmetics and

6 detergents [3,4,31-33].

7 Indeed the study of the behavior of salts in organic solvents stands out as a self

8 evidently important field of research because of the need for better insights into

9 the microscopic mechanisms that determine over specific ion phenomena. In

10 fact the way salts modify the structure and physico-chemical properties of

11 protic and aprotic polar liquids is of great importance to assess whether

12 hydrogen bonding is involved or not. Or indeed whether hydrogen bonding is a

13 meaningful or useful concept on which to build intuition and predictability.

14 The relative simplicity of aprotic solvents should contribute insights into of the

15 most significant problems related to the universality of Hofmeister effects in

16 aqueous solutions and dispersions, and to the elusive related issues of

17 hydrogen bond clusters and ion specificity of hydration interactions.

18 In this paper we specifically investigate the effect of HB on the solubility of

19 some salts and more particularly on the thermodynamics and other physico-

20 chemical properties through NMR, DSC and ATR-FTIR measurements. These

21 properties were studied in the presence of different potassium salts to elucidate

22 the interactions between the anions and the solvent. Since the solvent possesses

23 a terminal –OH group, it can establish HB in the pure liquid state, as suggested

24 and confirmed by several peculiar physico-chemical properties and

25 observations. The range of the investigated salts range from potassium halides

to phosphate, carbonate, sulfate and cyanate to study the effect of the anion's basicity and of the anion's capability to act as a donor/acceptor for hydrogen bonds. We found that fluoride, phosphate, carbonate and (partly) cyanate do behave as basic anions and are able to interact with the solvent molecules by participating in HB. Chloride and bromide play an intemediate role according to the Hofmeister sequence. Compared to the behavior of iodide in EC and PC, its interactions with GC represent a striking anomaly with respect to what we expected on the basis of our previous studies.

2 Experimental

2.1 Materials

Glycerol carbonate (≥90.0%), potassium fluoride (≥99.5%), potassium chloride (≥99.0%), potassium bromide (≥99.0%), potassium iodide (≥99.0%), potassium carbonate (≥99.0%), potassium phosphate (≥98.0%), potassium cyanate (96%), and potassium sulfate (≥99.0%) were purchased from Sigma-Aldrich (Milan, Italy). The salts were purified, dried and stored under vacuum, according to the standard procedures [3,4]. Glycerol carbonate was used as received and kept under inert atmosphere to avoid water contamination.

2.2 Solubility

The solubility of salts in GC was measured at different temperatures. A weighted amount of GC was transferred in a test tube and an excess of dry salt was added. The vial was sealed and kept under magnetic stirring for two days in a thermostatted bath at the required temperature (±0.1° C). The stirring was stopped and the saturated solution was left to equilibrate in the presence of the salt for 24 h, before a certain

amount (b, in grams) of solution was carefully taken from the top of the solution and transferred to a flask and diluted with water up to a volume V (in L). The aqueous mixture was than analysed through Inductively Coupled Plasma Atomic Emission Spectrometer (ICP-AES) in order to measure the concentration of K^+ (c, in mg/L). The calibration curve was built analysing five standard solutions of dry KCl using a water+GC mixture as a solvent with approximately the same composition of the sample under investigation. The calibration data were fitted with a quadratic curve with a correlation coefficient R^2 of 0.99993.

The solubility (m in molal units, *i.e.* moles of solute per 1 kg of GC) of the salt was then calculated as:

$$m = \frac{1000cV}{1000bM_K - cMV}$$

(1)

where M_K is the atomic mass of potassium (39.102 g/mol) and M is the molar mass of the salt.

2.1 Density of glycerol carbonate

The density of GC was measured with an Anton Paar DMA 5000 instrument as a function of temperature between 15° and 50° C, with an accuracy of $\pm 10^{-5}$ g/mL.

2.2 Nuclear Magnetic Resonance

1D- and 2D-NMR spectra were recorded with a Bruker 400 Ultrashield spectrometer operating at 400 MHz (for ^1H) and 100 MHz (for ^{13}C). All the experiments were carried out in vacuum-dried NMR coaxial tubes. $CDCl_3$ was used as external lock and reference material in the coaxial insert. NMR signals were referenced to nondeuterated residual solvent signals ($CDCl_3$, 7.26 ppm and 77.0 ppm for ^1H and ^{13}C, respectively). The monodimensional ^1H- and ^{13}C-NMR spectra for pure GC are shown in Figures S1 and S2 in the Supporting Information. The assignment of the chemical shift to each proton in the pure GC molecule was carried out by performing homo-

1 and heteronuclear 2D-NMR experiments as ^{1}H-^{1}H COSY (homonuclear correlation

2 spectroscopy) and ^{1}H-^{13}C HSQC (heteronuclear single quantum coherence

3 spectroscopy), see Figures S3 and S4 in the Supporting Information.

2.3 Differential Scanning Calorimetry

5 Differential Scanning Calorimetry (DSC) runs were carried out on a DSC-Q2000

6 from TA Instruments (Milan, Italy). The samples were first equilibrated at -30° C,

7 then cooled from –30 °C to –90° C at 2 °C/min, and finally heated up to -30° C at

8 2 °C/min. The experiments were conducted under N_2 atmosphere with a flow rate of

9 50 mL/min. The thermograms were analyzed by the TA Universal Analysis software.

10 For all samples the glass transition temperatures (T_g) were obtained from the

11 inflection point in the DSC signal.

2.4 Attenuated total reflection Fourier-transform infrared spectroscopy

13 Attenuated total reflection Fourier-transform infrared spectroscopy (ATR-FTIR)

14 spectra were acquired using a Thermo Nicolet Nexus 870 FT-IR spectrophotometer,

15 equipped with a liquid nitrogen cooled MCT (mercury-cadmium-telluride) detector,

16 by averaging on 128 scans at a resolution of 2 cm^{-1} and with CO_2-atmospheric

17 correction. The spectra were recorded between 4000 and 600 cm^{-1}. For each spectrum

18 the background was recorded and subtracted from the sample profile.

19

20 **3 Results and Discussion**

21 *3.1 Nuclear Magnetic Resonance*

22 The literature offers some reports on the effect of salts or ionic liquids on the NMR

23 spectra of organic molecules, and the study of Hofmeister phenomena by means of

24 NMR techniques is attracting an ever growing attention [34-40]. However a

1 systematic study on specific ion effects induced by a series of selected electrolytes on

2 the NMR spectral properties of glycerol carbonate has not been published yet.

3 NMR spectra were recorded on saturated solutions of KF, K_2CO_3, K_3PO_4, KCl, KBr,

4 KI, K_2SO_4 and KOCN in GC at room temperature. Figure 1 shows the NMR of pure

5 GC, and of its saturated solutions of different potassium salts. The individual spectra

6 are reported in the Supplementary Material (see Figures S1-S15).
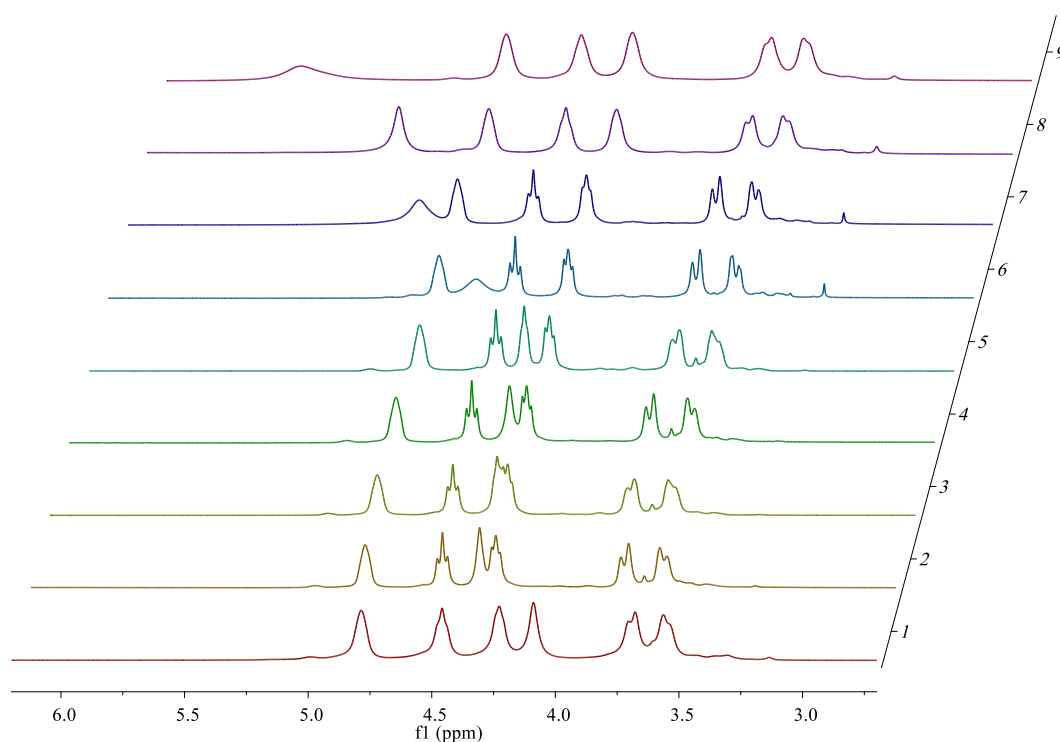
7

8 **Figure 1**. NMR spectra of pure GC and of its saturated solutions with different
9 potassium salts. 1: KI, 2: KBr, 3: pure GC, 4: K_2SO_4, 5: KCl, 6: K_2CO_3, 7: KCNO, 8:
10 K_3PO_4, 9: KF.
11

12 The change in the shift (δ) of the alcoholic proton was quantified through the shift

13 index I_S defined as:

14
$$I_S = 100 \frac{\delta_{sol} - \delta_0}{\delta_0} \qquad (2)$$

1 Where δ_0 (4.42 ppm) and δ_{sol} are the chemical shifts of the –OH in pure GC and in the

2 saturated salt solution, respectively. The values of I_S are reported in Table 2 and

3 follow the trend:

4 $$KF > K_3PO_4 > KOCN > K_2CO_3 > KCl > K_2SO_4 > KBr > KI$$

5 These results suggest that the major perturbation in the chemical shift of the –OH

6 proton is produced by anions that behave as strong bases: fluoride, carbonate,

7 phosphate, and cyanate. The deshielding of the hydrogen in the presence of these

8 anions indicates an electron-poor environment around this nucleus. These results

9 suggest that a quite strong interaction (hydrogen bonding) between the basic anion

10 and the -OH group takes place in saturated solutions of KF, K_2CO_3 and K_3PO_4.

11 **Table 2**. Chemical shift (δ, in ppm) and shift index ($I_S \pm 0.5\%$) of saturated solutions
12 of KF, KCl, KBr, KI, K_2CO_3, K_3PO_4, K_2SO_4 and KOCN. $CDCl_3$: $\delta = 7.26$ ppm.

salt	δ	I_S
(pure GC)	4.40	-
KF	5.66	28.6
K_3PO_4	5.18	17.7
KOCN	5.00	13.6
K_2CO_3	4.71	7.04
KCl	4.44	0.91
K_2SO_4	4.41	0.23
KBr	4.38	-0.34
KI	4.09	-7.05

13

14 This evidence parallels our previous findings that showed the presence of ion pairs,

15 triple ions and higher order clusters in saturated solutions of KF in GC through

16 viscosity and conductivity measurements [1]. A similar study on the viscosity and

17 conductivity of salt solutions in GC as a function of the solute concentration will be

18 performed in a future work in order to detect the presence of ion pairs and higher

19 clusters in GC salt solutions. After some time (about 30 hours) saturated solutions of

20 KF or K_3PO_4 slowly became yellowish due to the formation of 2,3-epoxy-1-propanol

21 (glycidol) and CO_2 [41].

1   On the other hand other anions such as chloride, sulfate and bromide do not alter

2   significantly the chemical environment around the alcoholic proton and/or the

3   structuredness of the solvent.

4   Concerning the non-hydroxyl protons, all salts left unaltered the NMR spectrum of

5   pure GC with the exception of KI, that produces a small but recordable change. In fact

6   the H_X and H_Y shift from 3.70-3.84 (in pure GC) to 3.56-3.70 ppm, between 2% and

7   4% compared to pure GC (see Table 3). Due to this effect we recorded HSQC spectra

8   on the GC+KI solution to double check the chemical shift and assignment of each

9   proton (see Figure S15 in the Supporting Information).

10   Remarkably, KI induces a strong decrement in the value of δ resulting in a negative

11   value of I_s. Since HI is a very strong acid and correspondingly iodide a very weak

12   base, this behavior is rather related to the large polarizability of this anion and to the

13   onset of significant dispersion interactions between the anion and the solvent

14   molecules. We recall that the polarizability of I^- in ethylene carbonate was calculated

15   to be as large as 3 $Å^3$ [3]. NMR spectra acquired on less concentrated solutions of the

16   same salts did not show any significant variation of the chemical shift respect to δ_0, in

17   fact a clear detectable change in the chemical shift was obtained using salt

18   concentrations near the solubility limit.

19   **Table 3**. Chemical shifts (δ, in ppm) of the non-hydroxyl protons (see Scheme 1) in
20   pure GC and in its saturated solution of KI.

	B,B′	C	D,D′
GC	3.70-3.84	4.88	4.35-4.57
KI	3.56-3.70	4.79	4.23-4.46

21

22   Noticeably potassium iodide lowered the chemical shifts of the non-hydroxyl protons

23   (between 2% and 4% respect to pure GC). The other investigated salts did not change

24   the δ of the same nuclei respect to pure GC. We argue that this shielding effect is

1 again due to the large polarizability of iodide that by approaching the GC ring creates

2 an electron-richer environment around these protons.

3 *3.2 Density*

4 The density of pure GC was measured as a function of temperature between 15° and

5 50° C (see Table 4).

6 A linear regression was used to fit the data:

7
$$\rho = 1.6750 - 9.4918 \cdot 10^{-4} T \tag{3}$$

8 **Table 4**. Density (ρ, in g/mL) of pure GC as function of temperature (T, in K). σ is
9 the standard deviation for each measured value. R = 0.99998.

$T(K)$	$\rho\,(g/mL)$	$\sigma\,(g/mL)$
288.0	1.4017	$1.7512 \cdot 10^{-6}$
293.0	1.3969	$5.0000 \cdot 10^{-7}$
298.0	1.3921	$1.2150 \cdot 10^{-6}$
303.0	1.3873	$8.3666 \cdot 10^{-7}$
308.0	1.3826	$1.2724 \cdot 10^{-6}$
313.0	1.3778	$9.8319 \cdot 10^{-7}$
318.0	1.3731	$9.8319 \cdot 10^{-7}$
323.0	1.3685	$8.9443 \cdot 10^{-7}$

10

11 *3.3 Solubility and thermodynamics of solvation*

12 The solubility of salts in GC at different temperatures was measured following the

13 same procedure adopted in previous studies [3,4]. We observed that potassium

14 phosphate, sulphate and carbonate behave similarly to KF [1], *i.e.* the solvent can be

15 easily oversaturated with these salts at all temperatures. In our previous study we

16 concluded that this behavior is related to the formation of very stable ion pairs, triple

17 ions (K_2F^+ and KF_2^-) and higher clusters, while the free K^+ and F^- ions represent only a

18 minor fraction of the entire distribution [1]. We also concluded that the ion pairs are

19 intercalated between solvent molecules through ion-dipole interactions between the

20 cation and the carbonyl moiety, and hydrogen bond between the anion and the

21 primary -OH residue. The NMR results reported in section 3.1 suggest that a similar

1   behavior ocurrs with phosphate, carbonate and cyanate. As a matter of fact K_3PO_4,

2   K_2CO_3 and KOCN can produce oversaturated solutions in GC.

3   Such behavior changes when the anion is unable to establish hydrogen bonds with the

4   solvent. Therefore we measured the solubility of KCl, KBr, KI and KOCN as a

5   function of temperature between 25° and 45° C. Table 5 reports the solubility of these

6   electrolytes expressed in molal units (*m*) in the equilibrated saturated solutions. The

7   solubility of all salts increases with the temperature, indicating that the dissolution

8   process is endothermic.

9   **Table 5**. Solubility (in molal units, mol/kg) of electrolytes in GC as a function of
10   temperature.

$T\,(°C)$	KCl	KBr	KI	KOCN
25°	$2.03 \cdot 10^{-3}$	$2.62 \cdot 10^{-3}$	$7.03 \cdot 10^{-3}$	$2.81 \cdot 10^{-3}$
30°	$4.45 \cdot 10^{-3}$	$5.30 \cdot 10^{-3}$	$13.4 \cdot 10^{-3}$	$3.66 \cdot 10^{-3}$
35°	$9.53 \cdot 10^{-3}$	$10.4 \cdot 10^{-3}$	$20.7 \cdot 10^{-3}$	$6.08 \cdot 10^{-3}$
40°	$19.0 \cdot 10^{-3}$	$19.6 \cdot 10^{-3}$	$24.6 \cdot 10^{-3}$	$14.4 \cdot 10^{-3}$
45°	$41.5 \cdot 10^{-3}$	$39.5 \cdot 10^{-3}$	$99.4 \cdot 10^{-3}$	$21.3 \cdot 10^{-3}$

11

12   From the experimental solubility the enthalpy, Gibbs free energy, and entropy

13   changes of solution can be calculated from equations 4-6 [42,43], assuming that in the

14   investigated temperature range they can be considered constant, and are listed in

15   Table 6:

16 $$\Delta_{sol}G^0 = -RTlnK_{sp} = -RTln(\gamma_{\pm}m)^2 \qquad (4)$$

17 $$\Delta_{sol}H^0 = -2R\left[\frac{\partial ln(\gamma_{\pm}m)}{\partial(1/T)}\right] \qquad (5)$$

18 $$\Delta_{sol}S^0 = (\Delta_{sol}H^0 - \Delta_{sol}G^0)/T \qquad (6)$$

19    $\gamma_{\pm}$ is the mean molal activity coefficient and K_{sp} the solubility product of the salt in

20   GC. The calculation of $\gamma_{\pm}$ is derived from the Debye-Hückel theory and the Bjerrum

21   formula, and outlined in the Appendix. However imperfect these theories may be, the

22   entropy changes are surely positive indicating that the addition of an electrolyte

23   induces a remarkable perturbation in the liquid structure.

1 The thermodynamic parameters obtained for GC suggest that the dissolution of the

2 electrolyte requires more energy than that involved in the orientation of the solvent

3 dipole around the dissolved ions.

4 **Table 6**. Enthalpy ($\Delta_{sol}H^0$, in kJ/mol), Gibbs free energy ($\Delta_{sol}G^0$, in kJ/mol), entropy
5 ($\Delta_{sol}S^0$, in J/K·mol) changes of solution at 30° C, lattice enthalpy (U, in kJ/mol), and
6 the experimental enthalpy change of solvation ($\Delta_{solv}H^0(exp)$, in kJ/mol) calculated
7 according to eq. 7 for the investigated electrolytes in GC.

salt	$\Delta_{sol}H^0$	$\Delta_{sol}G^0$	$\Delta_{sol}S^0$	U^a	$\Delta_{solv}H^0(exp)$
KCl	234	27	683	715	-481
KBr	208	26	600	682	-474
KI	203±8%	22	597	649	-446
KOCN	170±11%	28	468	653[b]	-483

8 a: see Ref. 44; b: calculated value.

9 The experimental enthalpy change of solvation, $\Delta_{solv}H^0(exp)$, was calculated as:

$$\Delta_{solv}H^0(exp) = \Delta_{sol}H^0 - U \tag{7}$$

11 where U is the lattice energy of each solid.

12 For a given ion the Gibbs free energy, the enthalpy, and the entropy changes of

13 solvation can be evaluated according to the modified Born theory that is basically an

14 electrostatic model [45]:

$$\Delta_{solv}G^0 = -\frac{e^2 N(\varepsilon-1)}{8\pi\varepsilon_0\varepsilon(r+\tau)} \tag{8}$$

$$\Delta_{solv}H^0 = -\frac{e^2 N}{8\pi\varepsilon_0(r+\tau)}\left(1 - \frac{1}{\varepsilon} - \frac{T}{\varepsilon^2}\frac{\partial\varepsilon}{\partial T}\right) \tag{9}$$

$$\Delta_{solv}S^0 = \frac{e^2 N}{8\pi\varepsilon_0\varepsilon^2(r+\tau)}\left(\frac{\partial\varepsilon}{\partial T}\right) \tag{10}$$

18 where e is the electron charge, ε the dielectric constant, ε_0 the vacuum permittivity, r_i

19 the crystal radius, T the absolute temperature and τ a fitting parameter. In the

20 derivation of ΔH and ΔS from the derivative of ΔG respect to the temperature, τ is

21 assumed to be temperature independent.

22 For GC, $\left(\frac{\partial\varepsilon}{\partial T}\right)$ is about -0.36 K^{-1}, and was estimated from the values of ε reported by

23 Chernyak [5].

1   The solvation thermodynamic parameters were calculated following the procedure

2   described in a previous work [3] and are listed in Table 7.

3   As with other polar solvents like dimethylformamide (DMF) or EC, the entropy of

4   solvation change of the ions in GC are all negative and small. Thus, the balance

5   between the disorder induced by the ion in the solvent and the re-ordering of the

6   solvation GC molecules around the ion brings about a (small) lowering in the entropy

7   [3]. The most effective re-structuring ion is K^+, while the anions have a smaller effect.

8   The values of $\Delta_{solv}S^0$ are quite similar to those that we calculated in ethylene

9   carbonate, indicating a similar perturbation in the liquid structure upon dissolution of

10   the salt [43].

11 **Table 7.** Calculated ion solvation free energy ($\Delta G_{solv}{}^{calc}$, in kJ·mol^{-1}), enthalpy ($\Delta_{solv}H^0$,
12 in kJ·mol^{-1}) and entropy ($\Delta_{solv}S^0$, in J·K^{-1}·mol^{-1}) changes (see equations 8-10) at 30° C,
13 crystallographic radius (r, in Å), experimental best fitting τ (in Å), for different ions
14 in glycerol carbonate.

Ion	$\Delta_{solv}G^0$	$\Delta_{solv}H^0$	$\Delta_{solv}S^0$	r	τ
K^+	-296	-300	-13	1.33	1.0
Cl^-	-181	-183	-7	1.81	2.0
Br^-	-174	-176	-7	1.96	2.0
I^-	-178	-180	-7	2.16	1.7
OCN^-	-179	-181	-7	2.34	1.5

15

16   As in the case of EC the solvation process is enthalpy driven and dominated by K^+,

17   while the solvation of anions is weaker (both in enthalpic and entropic terms).

18   Plotting the value of $\Delta_{solv}H^0$, calculated according to the Born equation [45] as a

19   function of the experimental value $\Delta_{solv}H^0(exp)$, we obtain the graph shown in Figure

20   2:

1
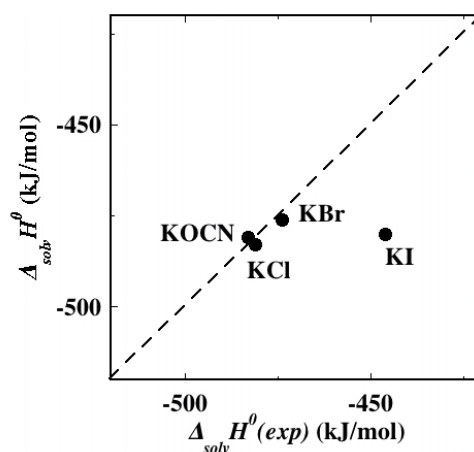
Figure 2. Calculated $\Delta_{solv}H^0$ versus experimental solvation enthalpy change $\Delta_{solv}H^0(exp)$ at 30° C for the investigated electrolytes in GC. The calculated value was obtained by summing the two contributions for the cation and the anion.

The calculated $\Delta_{solv}H^0$ was fitted to the Born equation, thus Figure 2 judges the goodness of that fit. The plot shows that the electrostatic Born model works quite well for all salts, except for KI for which there are significant deviations. This occurs also for ethylene carbonate [3]. The deviation is probably related to the non-electrostatic van der Waals interactions that iodide can establish with the solvent molecules due to its soft nature and large polarizability.

3.4 Differential Scanning Calorimetry

The thermal behavior of pure GC and of its saturated solutions was investigated through Differential Scanning Calorimetry (DSC). The DSC scans are reported in Figure 3. From the DSC experiments we detected a glass transition temperature (T_g) that strongly depends on the nature of the added salt (see Table 8).

Compared to pure GC (T_g = -70.8 °C), KF, K_3PO_4, KOCN and K_2CO_3 induce a significant increment in the glass transition temperature, while KCl, KBr and K_2SO_4 do not modify T_g in a significant manner. A similar behavior was reported for glycerol and PC [46,47]. The heat flow peak indicates the presence

1   of two contributions, the ΔC_p at the glass transition temperature (T_g), and the

2   endothermic peak related to the enthalpic recovery process. These can be

3   separated by a modulated DSC experiment.

4   **Table 8**. Glass transition temperature (T_g, in ° C) and wavenumber ($\bar{v}$ in cm^{-1}) for the
5   O-H stretching absorption in saturated solutions of salts in GC at 25° C.

salt	T_g	$\bar{v}$
(pure GC)	-70.8	3420
KF	-61.3	3370
K_3PO_4	-57.4	3398
KOCN	-58.5	3404
K_2CO_3	-62.8	3409
KCl	-70.4	3425
K_2SO_4	-70.0	3428
KBr	-66.5	3408
KI	-61.5	3372

6

7   The large increment in the T_g of the liquid upon the addition of KF, K_3PO_4,

8   KOCN and K_2CO_3 confirms a strong stiffening effect induced by the electrolyte

9   on the solvent molecules structuredness as outlined in our previous work [1].

10   Unexpectedly, KI has the same effect as KF on the glass transition temperature

11   of liquid GC, although it is not able to bind to the –OH group as do the basic

12   anions. We argue that this result and the shielding effect induced by I$^-$ on the

13   protons of the ring may be explained by invoking a partial approach of I$^-$

14   toward the glycerol carbonate's ring due to non-electrostatic van der Waals

15   forces that involve this anion and the solvent molecules. Probably this

16   phenomenon perturbs the structuredness, reduces the mobility of the solvent

17   molecules and hence increases the glass transition temperature [48]. Further

18   studies are necessary to detail the specific mechanism through which these

19   phenomena occur.
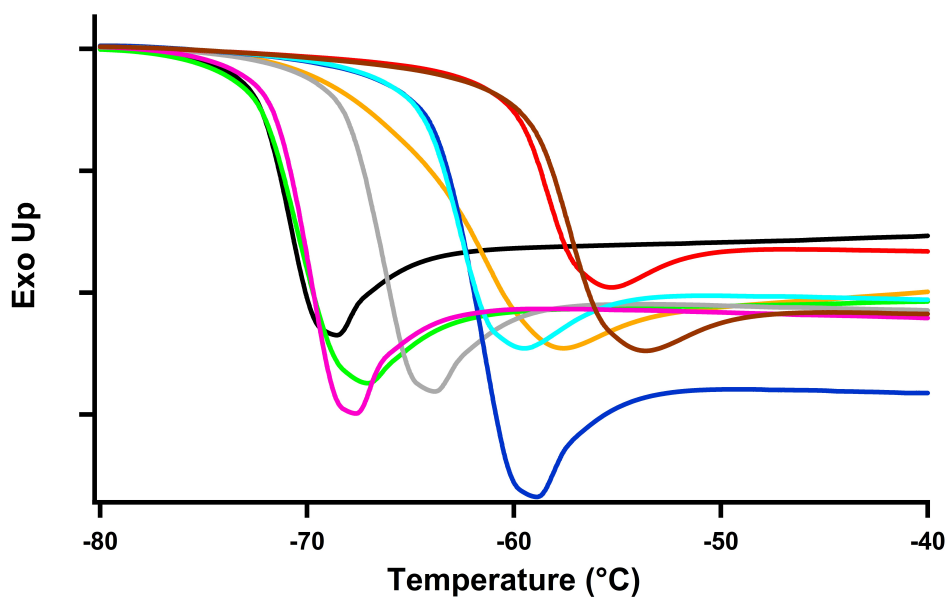
Figure 3. DSC curves for pure GC (black), KF (orange), KCl (green), KBr (grey), KI (dark blue), KOCN (red), K_2CO_3 (light blue), K_2SO_4 (pink) and K_3PO_4 (brown) saturated solutions.

3.5 Attenuated Total Reflection-Fourier Transform Infrared Spectroscopy

The Attenuated Total Reflection-Fourier Transform Infrared Spectroscopy (ATR-FTIR) experiments indicate a shift of the O-H stretching band from the pristine 3420 cm^{-1} wavenumber that was found for pure GC (see Table 8). The lowering in the frequency of the O-H signal induced by the presence of KF, K_3PO_4, KOCN and K_2CO_3 reflects the interaction between the hydroxyl moiety and the basic anion, that leads to a weakening in the O-H stretching mode. KI produces an effect comparable to that of KF with a significant shift (from 3420 to 3370 cm^{-1}) in the O-H stretching, indicating a weakening in the strength of the O-H bond. This result parallels the effect that we already recorded in NMR and DSC experiments on KI+GC samples and can be related to the partial adsorption of iodide ions near the GC ring.

4 Conclusion

The results indicate the dissolution of an electrolyte in glycerol carbonate occurs via two different solvation mechanisms. On one hand the potassium cation interacts with the carbonyl group through simple electrostatic ion-dipole interactions. On the other hand the role played by the anion greatly depends on its nature. If the anion has a strong basic nature, then it interacts with the hydroxyl moiety through hydrogen bonding. This would modify the structuredness of the solvent significantly. Instead, if the anion is not an acceptor, then its interaction with the solvent molecule is minimal. However, in the case of iodide, we recorded a peculiar behavior reminiscent of the effect induced by the very basic fluoride anion. Taking into account the large static polarizability of GC, we discussed this ~~iodide~~ anomaly in terms of polarizability-related non-electrostatic van der Waals interactions that brings the anion close to the GC ring.

In conclusion, if the anion behaves as a strong base in a protic solvent, then the formation of hydrogen bonding is the main feature that determines the behavior of the salt in the solution. On the other hand when the anion cannot participate in a hydrogen bond, then other kinds of interactions, such as van der Waals non-electrostatic forces are at play and in this case specific ion effects emerge. As a natural extension of this work we envisage the study of the effect induced by more salts (including nitrate, thiocyanate, perchlorate, chlorate, tetrabutylammonium, tetraphenylborate, etc.), the experimental measurements of the activity coefficient, and the acquisition of SAXS profiles on GC solutions in the presence of different salts. We are confident that the new

Appendix A. Mean molal activity coefficient.

The mean molal activity coefficient for the free ions ($\gamma_\pm$) was estimated through the Debye-Hückel theory as [3,49]:

$$log\gamma_\pm = -\frac{A\sqrt{m}}{1+Ba\sqrt{m}} \tag{A1}$$

Here m is the molal concentration of the salt.

$$A = 1.8247 \cdot 10^6 \sqrt{\frac{\rho}{\varepsilon^3 T^3}} \tag{A2}$$

$$B = 50.2901 \sqrt{\frac{\rho}{\varepsilon T}} \tag{A3}$$

where ρ, ε_r and T are the density and the static dielectric constant of the solvent, and the absolute temperature, respectively. A is in kg$^{1/2}$·mol$^{-1/2}$ and B in kg$^{1/2}$·mol$^{-1/2}$·Å^{-1}. a is the distance of closest approach. For fully dissociated 1:1 electrolytes a can be taken as the Bjerrum length q:

$$q = \frac{e^2}{2\varepsilon k_B T} \tag{A4}$$

where e and k_B are the elementary charge and the Boltzmann constant, respectively.

Table A1 shows the values of ε_r, A, q, and B as a function of temperature that were used for the calculation of the average ionic activity coefficients in GC solutions (see Table A2).

Table A1. Values of ε, A, q, and B as a function of temperature used for the calculation of $\gamma_\pm$ in GC solutions.

T	ε	A	q	B
25.1	109.6	0.3642	2.5558	0.3281
30.1	107.8	0.3635	2.5556	0.3276
35.1	106.0	0.3632	2.5569	0.3271
39.7	104.3	0.3631	2.5593	0.3267

45.0	102.4	0.3633	2.5635	0.3264

Table A2. Values of $\gamma_{\pm}$ for the different salts in GC as a function of temperature according to eqs. A1-A4.

T	$\gamma_{\pm}$ (KCl)	$\gamma_{\pm}$ (KBr)	$\gamma_{\pm}$ (KI)	$\gamma_{\pm}$ (KOCN)
25.1	0.99158	0.98354	0.97187	0.98167
30.1	0.98294	0.97113	0.96241	0.97928
35.1	0.97616	0.96349	0.95443	0.97377
39.7	0.95875	0.93207	0.95093	0.96114
45.0	0.92919	0.90071	0.91333	0.95380

References

[1] F. Sarri, D. Tatini, M. Ambrosi, E. Carretti, B.W. Ninham, L. Dei, P. Lo Nostro, J. Mol. Liq. 255 (2018) 397.

[2] V. Mazzini, V.S.J. Craig, Chem. Sci. 8 (2017) 7052.

[3] N. Peruzzi, B. W. Ninham, P. Lo Nostro, P. Baglioni, J. Phys. Chem. B 116 (2012) 14398

[4] N. Peruzzi, P. Lo Nostro, B. W. Ninham, P. Baglioni, J. Sol. Chem. 44 (2015) 1224.

[5] Y. Chernyak, J. Chem. Eng. Data 51 (2006) 416.

[6] M.O. Sonnati, S. Amigoni, E.P. Taffin de Givenchy, T. Darmanin, O. Choulet, F. Guittard, Green Chem. 15 (2013) 283.

[7] C.S. Hong, R. Wakslak, H. Flnston, V. Fried, J. Chem. Eng. Data 27 (1982) 27, 146.

[8] M.S. Ding, J. Chem. Eng. Data 49 (2004) 276.

[9] S.P. Verevkin, A.V. Toktonov, Y Chernyak, B. Schäffner, A. Börner, Fluid Phase Equilib. 268 (2008) 1.

1   [10]   Y. Nannoolal, J. Rarey, J. Ramjugernath, J. Fluid Phase Equilib. 252 (2007) 1.

2   [11]   R. Naejus, C. Damas, D. Lemordant, R. Coudert, J. Chem. Thermodynamics

3   34 (2002) 795.

4   [12]   R. Bosque, J, Sales, J. Chem. Inf. Comput. Sci. 42 (2002) 1154.

5   [13]   S. Nir, S. Adams, R. Rein, J. Chem. Phys. 59 (1973) 3341.

6   [14]   P. Lo Nostro, B.W. Ninham, Chem. Rev. 112 (2012) 2286.

7   [15]   B.W. Ninham, R.M. Pashley, P. Lo Nostro. Curr. Opin. Colloid Interface

8   Sci. 27 (2016) 25.

9   [16]   T. Duignan, D.F. Parsons, B.W. Ninham, J. Phys. Chem. B 118 (2014) 3122.

10 [17]   T. Duignan, D.F. Parsons, B.W. Ninham, Chem. Phys. Lett. 635 (2015) 1.

11 [18]   B.W. Ninham, P. Lo Nostro, Water, salt and oil. An exploration of the

12   foundations of molecular forces in "Aqua Incognita: Why Ice Floats on Water

13   and Galileo 400 Years on", P. Lo Nostro and B. W. Ninham Eds. Connor

14   Court Publishers, Ballarat, 2014, 103-126.

15 [19]   B.W. Ninham, Substantia 1 (2017) 7.

16 [20]   P. Lo Nostro, B.W. Ninham, Curr. Opin. Colloid Interface Sci. 23 (2016) A1.

17 [21]   D.F. Parsons, M. Boström, P. Lo Nostro, B.W. Ninham, Phys. Chem. Chem.

18   Phys. 13 (2011) 12352.

19 [22]   B.W. Ninham, R.A. Sammut, J. Theor. Biol. 56 (1976) 125.

20 [23]   X.N. Ying, Phys. Scr. 88 (2013) 025603.

21 [24]   U.R. Pedersen, P. Harrowell, J. Phys. Chem. B 115 (2011) 14205.

22 [25]   K. Koperwas, K. Adrjanowicz, Z. Wojnarowska, A. Jedrzejowska, J.

23   Knapik, M. Paluch, Sci. Rep. 6 (2016) 36934.

24 [26]   R.Zondervan, T. Xia, H. van der Meer, C. Storm, F. Kulzer, W. van

25   Saarloos, M. Orrit, Proc. Natl. Acad. Sci. USA 105 (2008) 4993.

1   [27]   M. Köhler, P. Lunkenheimer, A. Loid, Eur. Phys. J. E 27 (2008) 115.

2   [28]   P.U. Okoye, A.Z. Abdullah, B.H. Hameed, J. Taiwan Inst. Chem. E. 68 (2016)

3   51.

4   [29]   P.U. Okoye, A.Z. Abdullah, B.H. Hameed, Energ. Convers. Manage. 133

5   (2017) 477.

6   [30]   Y.M. Delavoux, M. Gilmore, M.P. Atkins, M. Swadzba-Kwasny,   J.D.

7   Holbrey, Phys. Chem. Chem. Phys. 19 (2017) 2867.

8   [31]   Z. Zhang, D.W. Rackemann, W.O.S. Doherty, I.M. O'Hara, Biotechnol.

9   Biofuels 6 (2013) 153.

10 [32]   M. Pagliaro, R. Ciriminna, H. Kimura, M. Rossi, C. Della Pina, Angew.

11   Chem. Int. Ed. 46 (2007) 4434.

12 [33]   J.R. Ochoa-Gómez, O. Gómez-Jiménez-Aberasturi, C. Ramírez-López, M.

13   Belsué, Org. Process Res. Dev. 16 (2012) 389.

14 [34]   A. Strate, V. Overbeck, V. Lehde, J. Neumann, A. M. Bonsa, T. Niemann, D.

15   Paschek, D. Michalik, Ralf Ludwig, Phys. Chem. Chem. Phys. 20 (2018)

16   5617.

17 [35]   N.O. Johnson, T.P. Light, G. MacDonald, Y. Zhang J. Phys. Chem. B 121

18   (2017) 1649.

19 [36]   C. Wiedemann, O. Ohlenschläger, C. Mrestani-Klaus, F. Bordusa Phys. Chem.

20   Chem. Phys. 19 (2017) 24115.

21 [37]   J.W. Bye, N.J. Baxter, A.M. Hounslow, R.J. Falconer, M.P. Williamson, ACS

22   Omega 1 (2016) 669.

23 [38]   G. Bekçioğlu-Neff, C. Allolio, Y.S. Desmukh, M. Ryan Hansen, D.

24   Sebastiani, ChemPhysChem 17 (2016) 1166.

25 [39]   J. Shi, J. Wang, J. Phys. Chem. B 118 (2014) 12336.

26 [40]   L.I.N. Tomé, F.R. Varanda, M.G. Freire, I.M. Marrucho, J.A.P. Coutinho, J.

27   Phys. Chem. B 113 (2009) 2815.

1   [41]   D.J. Darensbourg, A.D. Yeung, Green Chem. 16 (2014) 247.

2   [42]   J. Strong, T.R. Tuttle, J. Phys. Chem. 77 (1972) 533.

3   [43]   C.M. Criss, E. Luksha, J. Phys. Chem. 72 (1968) 2966.

4   [44]   C.R. Gopikrishnan, D. Jose, A. Datta, AIP Adv. 2 (2012) 012131.
5
6   [45]   M. Salomon, J. Phys. Chem. 74 (1970) 2519.

7   [46]   A.G. Lyapin, E.L. Gromnitskaya, I.V. Danilov, V.V. Brazhkin, RSC Adv. 7

8   (2017) 33278.

9   [47]   J. Geschwind, H. Frey, Macromolecules 46 (2013) 3280.

10 [48]   J.M.G. Cowie, V. Arrighi, Polymers: Chemistry and Physics of Modern

11   Materials, 3rd edition, CRC Press, Boca Raton, 2007.

12 [49]   F. Hernández-Luis, M.V. Vazquez, M.A. Esteso, Fluid Phase Equilib. 218

13   (2004) 295.